Transition Between Molten-Salt and Solvated-Ion States of Proton Hydrates: Comparative Double-Layer and Electrode-Kinetic Behaviour at Hg and Au Interfaces

S. Y. Qian* and B. E. Conway

Chemistry Department, University of Ottawa, Ottawa, Ontario, Canada

Z. Naturforsch. **46a**, 160–173 (1991); received June 5, 1990

Dedicated to Dr. K. Heinzinger on the ocassion of his 60th birthday

The question of the structure of the electrical double-layer at electrodes in contact with electrolyte solutions has several aspects in common with the long and short-range structure of electrolyte solutions. Measurements of the capacitance of the double-layer have traditionally provided information on this question for the case of dilute electrolyte solutions.

With proton hydrates from H_3O^+ through $H_9O_4^+$ to 1 M aqueous H^+ solution made by stoichiometric addition of water to the acid CF_3SO_3H, the transition between "molten-salt" ($H_3O^+ \cdot CF_3SO_3^-$ above 307 K) to "dilute-solution" behaviour of the interphasial double-layer at Hg and Au electrodes can be investigated. The $H_3O^+ \cdot CF_3SO_3^-$ is a highly conducting molten salt above 307 K. The results indicate that the double-layer capacitance at potentials negative to the RHE, both at Hg and Au, in the H_3O^+ molten salt has values surprisingly similar to that in 1 M aq. H^+ solution. Intermediate states of hydration of the proton ($H_5O_2^+$, $H_7O_3^+$, $H_9O_4^+$) have higher values, especially at Au. However, the capacitance behaviour is quite different from that observed in high-temperature, alkali-metal molten salts at Pb.

Models are proposed for the structures of the double-layers in these proton-hydrate systems, and the problem of accounting for a "normal" value (ca. 18 $\mu F\ cm^{-2}$) of capacitance at Hg in the H_3O^+ melt is examined by means of some model calculations.

Comparative electrode-kinetic measurements on proton discharge add further information on the behaviour of the proton hydrates.

Introduction

The short- and long-range structure of the electrical double-layer at electrode interfaces bears several similarities to that in solutions of electrolytes [1]. At the interface of electrodes there is a nearest-neighbour solvation layer of water molecules oriented, as at ions, to an extent determined by the charge-density, q, at the interface [2–4] and the corresponding local field. Additionally, there is a layer of electrostatically bound anions or cations [5] (analogous to ion pairing in electrolytes) depending on the sign of q; in the case of anions, the adsorption is often chemisorptive with partial charge-transfer between the ad-ion and the electrode metal [5–7]. Conjugate to the adion layer (Helmholtz planes [5]) is a diffuse ionic atmosphere [7] as with 3-dimensional distributions of ions in electrolyte solutions.

The Gibbs energy of hydration or solvation is one of the principal factors determining the extent to which chemisorption of ions takes place with partial charge-transfer [6, 8, 9] at an electrode; it also determines [10, 11], in part, but in a most important way, the activation energy for ion discharge associated with the coupled process of desolvation of the ion.

Extensive work is to be found in the literature [12–14] on both the problem of structure of electrolyte solutions, especially including that of the solvents themselves (in the case of H_2O and CH_3OH), and that of interfaces with liquids and electrolyte solutions. Some of this work was informative but empirical in nature [13]. Major improvements have been made in recent years towards in *ab initio* representation of the structures of liquids [16], ionic solutions [12] and liquid/solid interfaces [15] especially in the molecular dynamics calculations of Heinzinger and his colleagues, as referenced incompletely above. For electrochemistry and solution chemistry, his MD calculations of the positional and orientational distributions of hydrating H_2O molecules in the first coordination shells of ions of various charge densities, his evaluations of

* Visiting Scholar from the Peoples Republic of China.

Reprint requests to Prof. B. E. Conway, Chemistry Department, University of Ottawa, 32 George Glinski Street, Ottawa, Ont. K1N 6N5, Canada.

0932-0784 / 91 / 0100-0160 $ 01.30/0.

radial distributions for the structure of water and his treatment of the distribution of liquid-phase molecules at/near a wall, have been of particular value.

The proton has been recognized as playing a major role in chemistry and electrochemistry. In particular, the state of the *hydrated proton* in solution has attached special interest not only from the point of view of electrochemistry but in relation to the physical chemistry of acidity and conductance of acid solutions. Elsewhere this question has been considered [17, 18] and reviewed [19, 20] with regard to the existence of H_3O^+ itself and characterization of higher states of hydration [21] of H^+. Well defined states of hydration and solvation of the proton have also been observed in the vapour phase, and their speciations and stabilities determined, mainly by mass-spectrometry [32].

Purpose and Scope of the Work

The purpose of the present work is to examine the progression of the structure of the interfaces between Hg, and comparatively at Au, with a series of states of the hydrated proton that can be experimentally realized between the stoichiometry H_3O^+, through time-average stoichiometries $H_5O_2^+$, $H_7O_3^+$, $H_9O_4^+$ (cf. [21]) to that corresponding to H^+ (aq.), i.e. in dilute aqueous solution. The measurements involve determinations of the interfacial capacitance of Hg and Au electrodes, over a range of potentials, in contact with the melt $H_3O^+ \cdot CF_3SO_3^-$, where the state of H^+ as the H_3O^+ molecule-ion is well defined, through $H_9O_4^+ \cdot CF_3SO_3^-$ (*ca.* 14 molal) to a regular aqueous solution of the strongly dissociated acid CF_3SO_3H in water at 1.0 M concentration. The three hydrates of H^+, beyond H_3O^+, will be in the state of solvent-separated ion pairs and there will presumably be rapid proton mobility within the hydrate structures, as for the case of $H_9O_4^+$ specifically considered in the literature [21]. At Hg, in dilute aq. solution, the structure of the double-layer is well understood [3, 5, 7].

The experiments to be described in this paper are made possible by the opportunity that the pure acid CF_3SO_3H provides, of forming its "monohydrate" [22], which is actually the salt $H_3O^+ \cdot CF_3SO_3^-$, and which can be prepared in a highly purified form by vacuum distillation and crystallization (m.p. 307 K). Other nominal states of hydration can be prepared by appropriate provision of 1, 2 or 3 further molecules of water to the H_3O^+ salt. The CF_3SO_3H/H_2O system is also of practial interest as an acid fuel-cell electrolyte having advantageous properties for the O_2-cathode process.

With the $H_3O^+ \cdot CF_3SO_3^-$ salt, electrochemical measurements can be made just above the m.p. so that the behaviour of a room-temperature molten salt of the H_3O^+ ion can be compared with that of solutions of other states of the hydrated proton up to H^+ (aq.) in dilute solution. This provides the opportunity, amongst other things, of comparing the interfacial capacitance of a molten salt at Hg and Au with that of a dilute solution and of intermediate hydrate states of the proton. The double-layer capacitance behaviour at Hg and Au in the low-temperature H_3O^+ melt can also be compared with that at a Pb electrode in molten NaCl/KCl melts studied at elevated temperatures by Ushke et al. [23].

At Au, these experiments for various CF_3SO_3H/H_2O compositions, enable the interfacial capacitance to be evaluated both at potentials positive to the RHE just prior to Au surface oxidation, and at negative potentials, in the cathodic H_2 evolution region. This enables the state of the interface at which proton transfer occurs to be characterized from a "molten-salt" configuration [22] to a regular Stern-Grahame configuration [5, 7] in excess water.

Corresponding kinetic experiments on proton discharge enable the exchange current-densities, i_0, the heats of activation ΔH^+ (corrected for variation of the reference electrode potential with temperature from non-isothermal cell measurements) and, in particular, the variation of the Tafel slope, b, with temperature (cf. [24, 25]) to be determined, thus adding some further data for new systems with regard to temperature dependence of the transfer coefficient α or the barrier symmetry factor, β (cf. [26]).

In the present paper we examine how the state of hydration of the proton and its conjugate anion, $CF_3SO_3^-$, in trifluoromethane sulphonic acid solutions and in the "room-temperature" melt [21], $H_3O^+ \cdot CF_3SO_3^-$, affects the interfacial capacitance behaviour of mercury and gold electrodes and the kinetics of proton discharge at this metal. Previously, we demonstrated [22] that cathodic H_2 evolution could be studied from the $H_3O^+ \cdot CF_3SO_3^-$ melt and determined the enthalpic (β_H) and entropic ($T\beta_S$) components of the barrier symmetry factor ($\beta = \beta_H + T\beta_S$, cf. [24–26]) for this process at the Hg electrode in aqueous and methanolic solutions where the simple proton discharge event is rate-controlling.

The results obtained in the present work allow the transition between "molten-salt" to "ionic-solution" behaviour to be investigated, both kinetically and with respect to the double-layer capacitance behaviour at metal/molten H_3O^+ salt and metal/proton-hydrate interfaces.

Experimental

Methods: The interfacial capacitance behaviour of liquid Hg over a range of potentials and at polycrystalline Au electrodes at potentials both positive and negative to the RHE in the same medium was determined in the $H_3O^+ \cdot CF_3SO_3^-$ melt and in the other liquid proton hydrate media through to 1 M aqueous solutions of CF_3SO_3H (see below) as a function of potential on the positive side by cyclic-voltammetry and from a small-amplitude (7 mV) linear potential sweep at 35 mV s^{-1} superimposed on a series of potential steps of 50 mV. The response currents gave the required interfacial capacitance behaviour over the potential sweeps at the controlled potentials of the sequential steps.

The instrumental arrangement consisted of an Hokuto Denko potentiostat commanded by a PAR function generator. This system was also employed to record point-by-point current vs. potential relations for cathodic H_2 evolution at Hg and Au, using an on-line minicomputer. This procedure, as used previously [27], ensured very reproducible kinetic results.

At potentials negative to the RHE, the capacitance was determined by means of a.c. impedance and potential-relaxation methods. At Hg, the a.c. impedance behaviour is excellently represented by virtually perfect semicircles in the complex-plane plots of the real (Z') vs. the imaginary (Z'') components of the impedance vector. There is no anomalous dispersion corresponding to depression of the centre of the semicircle below the Z' axis as arises at some solid electrodes. The C values can therefore be reliably evaluated.

Technique and Apparatus: All experiments were performed in a thermostated all-glass, 3-compartment cell, using high-purification techniques as described in earlier papers [28, 29].

Electrodes: a) Aldrich Gold Label high-purity Hg was used as a recumbent Hg electrode formed in a glass cup connected to a 1 mm Pyrex capillary joined to an electrical contact and a micrometer syringe. The capillary and cup had been previously silanized to prevent creep of electrolyte below the meniscus, as in other works in the literature. This procedure led to excellently reproducible results. The silanization procedure was repeated, as necessary, at various intervals.

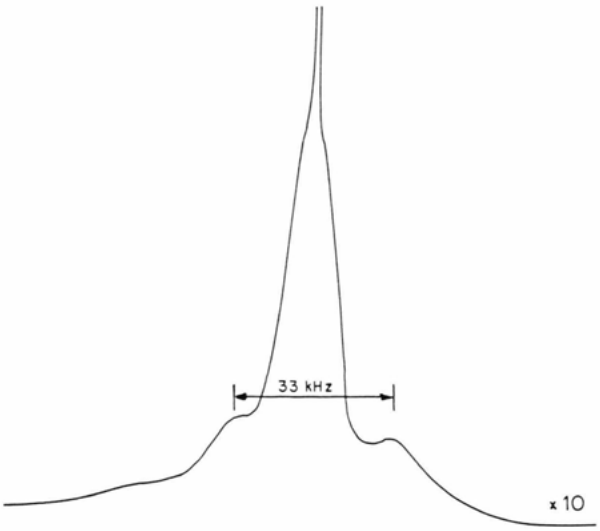

Fig. 1. Pulsed 300 MHz ^1H NMR spectrum of H_3O^+ in solid $H_3O^+ \cdot CF_3SO_3^-$ at 298 K (pulse time 3 μs, 287 acquisitions).

b) Polycrystalline 99.99% pure Au wires from Johnson Matthey were used in the solid-electrode work, with the Au being sealed into soft-glass electrode holders with a spot-welded Ag wire contact to the external circuit. After washing in acetone and pyrodistilled water [29], the Au electrodes were cycled several times in the acid solution at 25 mV s^{-1} between 0.05 and 1.5 V, RHE, to establish an electrochemically clean and reproducible surface.

An H_2/Pt or β-PdH electrode in the same solution as the Hg or Au electrodes was used as the reference electrode.

Electrolytes and Solutions: $H_3O^+ \cdot CF_3SO_3^-$ was prepared from redistilled CF_3SO_3H followed by treatment with a stoichiometric mole of H_2O. The resulting acid salt, $H_3O^+ \cdot CF_3SO_3^-$ (see Results Section), was then distilled *in vacuo* and collected in glass ampoules which were then sealed until used in the electrochemical interfacial capacitance and H_2-kinetic experiments. The acid salt has a m.p. of 307 K and gave a "good quality" cyclic-voltammogram at Au without any indications of effects of impurities in

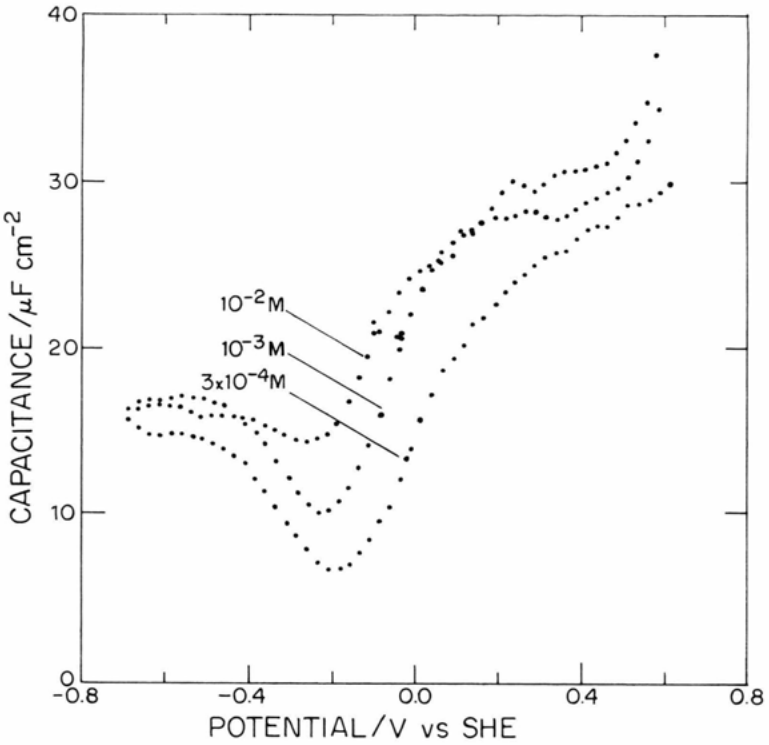

Fig. 2. Double-layer capacitance vs. potential profiles for Hg at 313 K in 3×10^{-4}, 10^{-3}, and 10^{-2} M aq. CF_3SO_3H solutions (strongly dissociated to $H^+_{aq} + CF_3SO_3^-$ ions).

the melt or on the Au surface (cf. [29] and [30]); it also gave the 3-peak solid-state proton n.m.r. spectrum (Fig. 1) characteristic of the structure $H_3O^+ \cdot CF_3SO_3^-$ rather than the monohydrate $CF_3SO_3H \cdot 1\,H_2O$ (cf. [31]).

Aqueous solutions of redistilled CF_3SO_3H were made up accurately in pyrodistilled water [29] to give also nominal compositions corresponding to the proton hydrate species $H_5O_2^+$, $H_7O_3^+$ and $H_9O_4^+$ (cf. [21] and [32]), and to 1 M aq. solution.

Results and Discussion

1. Introduction

Results will be presented for Hg electrodes at 298 K and compared, in a later section,with those obtained under similar conditions at the non-electrocatalytic solid electrode, Au. Thus, in many ways, Au, as a solid metal, provides a basis for comparison with the liquid metal (298 K) Hg since both have filled 4f and 5d electron shells, and 1 and 2 electrons, respectively, in the 6s valence electron sub-shell. Neither electrode exhibits any significant H chemisorption in cathodic H_2 evolution, indicating a rate-controlling proton-discharge step in that process (cf. [33] and [34]).

2. Capacitance Behaviour at Hg in the Proton Hydrates

It is well known (e.g. [5]) that in sufficiently strong electrolyte solutions, as is the case there, the measured double-layer capacitance, C, represents, to a good approximation, the compact double-layer capacitance, C_c, since the diffuse-layer capacitance, C_d, in the reciprocal relation $C^{-1} = C_c^{-1} + C_d^{-1}$ is $\gg C_c$. Hence C provides values of the compact-layer capacitance which gives information on the short-range geometry and structure of the interphase. In the species of systems of proton hydrates studied in the present work, this structure will change from that corresponding to a distribution of H_3O^+ cations and $CF_3SO_3^-$ anions with supposedly *no* free water present, through structures involving hydrated H_3O^+ and $CF_3SO_3^-$ ions with varying quantities of associated or free water.

Figure 2 shows that for dilute aqueous solutions of CF_3SO_3H (fully dissociated as H^+ aq. + $CF_3SO_3^-$ aq.) the interfacial capacitance for Hg is of the expected

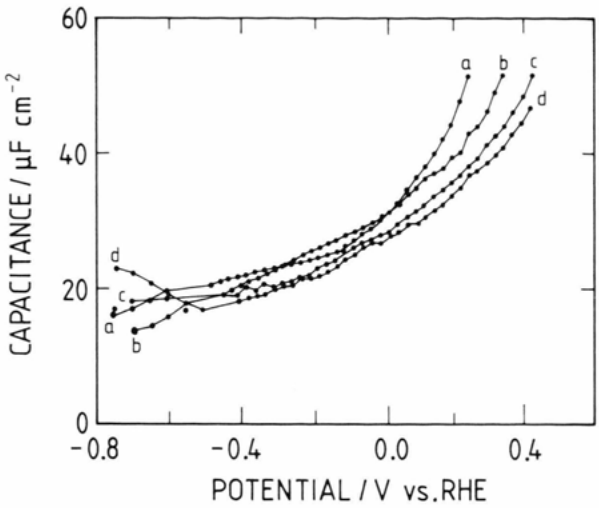

Fig. 3. Capacitance vs. potential profile for the Hg-pool electrode in $H_3O^+ \cdot CF_3SO_3^-$ (a), $H_5O_2^+ \cdot CF_3SO_3^-$ (b), $H_7O_3^+ \cdot CF_3SO_3^-$ (c) and $H_9O_4^+ \cdot CF_3SO_3$ (d) at 313 K, determined by small-amplitude cyclic linear sweeps superimposed on a successive potential-step programme of potential change.

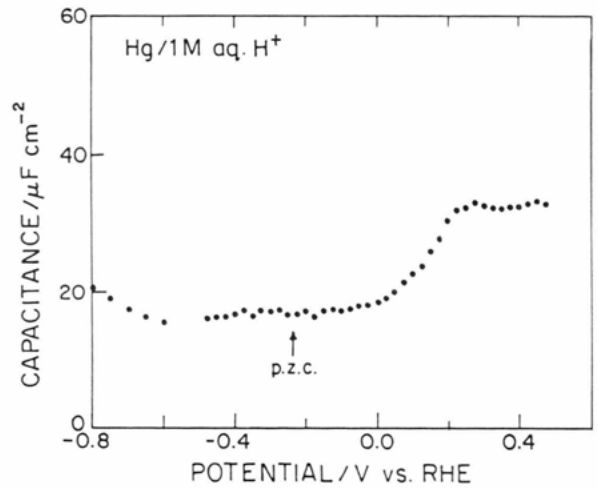

Fig. 4. As in Fig. 3, but for 1 M aq. $H^+ \cdot CF_3SO_3^-$. p.z.c. = potential of zero change.

(cf. [5]) form with a capacitance minimum at the potential of zero charge (p.z.c.) around which C_d no longer greatly exceeds C_c. In Fig. 2, the capacitance behaviour for 3×10^{-4} M, 10^{-3} M and 10^{-2} M solutions is shown.

The capacitance behaviour at Hg, as a function of potential, for four proton hydrate trifluoromethane sulphonates, H_3O^+ to $H_9O_4^+$ is shown in Fig. 3 and for 1 M aq. solution in Fig. 4 for comparison. The behaviour for the latter solution does not, of course, exhibit a minimum (cf. Fig. 2) since $C_d \gg C_c$ for such concentrations.

Note that if these curves of Figs. 3 and 4 were to be compared as a function of potential vs. SHE they would be appreciably displaced laterally on the potential scale due to the large proton activity (or mean acid activity) differences from H_3O^+ in the melt, through the proton hydrates, to approximately unit activity in the 1 M aq. acid solution.

A comparatively view of the capacitance behaviour at Hg for the five states of the hydrated proton is shown in Fig. 5. Here it is seen that the main differences of significance arise at potentials negative to the p.z.c. This is as expected since, at such potentials, the proton hydrate cations predominantly populate the compact layer. The lowest capacity arises with the H_3O^+ molten salt, where the distance of closest approach to the Hg surface for negative values of q will be determined by the radius of H_3O^+ while, for higher hydrates, this factor will be larger, tending to give rise to lower compact layer capacitances owing to a thicker compact layer. The effect is, however, evidently outweighted by a smaller dielectric constant due to absence of free H_2O molecules.

Formally, $C_c = \varkappa_0 \varepsilon_c / 4\pi d$, where ε_c is the dielectric constant of the compact layer region, $\varkappa_0$ the permittivity of vacuum and d the effective dielectric thickness of the compact region of the interphase. With increasing extent of hydration of H^+ in the interphase, both ε_c and d will tend to increase, so C_c can either increase or decrease with changing degree of hydration of H^+.

The variation of C_c for Hg with the increase of hydration, expressed as different hydrate species from H_3O^+ through $H_9O_4^+$ to 1 M aq. H^+, is shown in Figs. 6a, b, c for the three cathodic potentials from which it is seen that, in fact, there is a significant maximum and minimum in C_c as a function of the proton speciation. These variations of C_c by about 5 to 8 μF cm^{-2} are well outside the possible error, Δ, of measurement of C_c which is ca. $\Delta C_c = 0.5$ μF cm^{-2} except at extremes of the "d.c." polarization potentials. The variations of C_c are therefore experimentally significant for the dependence of structure of the double-layer at Hg on extent of proton hydration and water dipole orientation [2, 3].

It is to be noted from Fig., 6 that the maxima or minima in the dependence of C_c on speciation do depend significantly on the potential; this must be

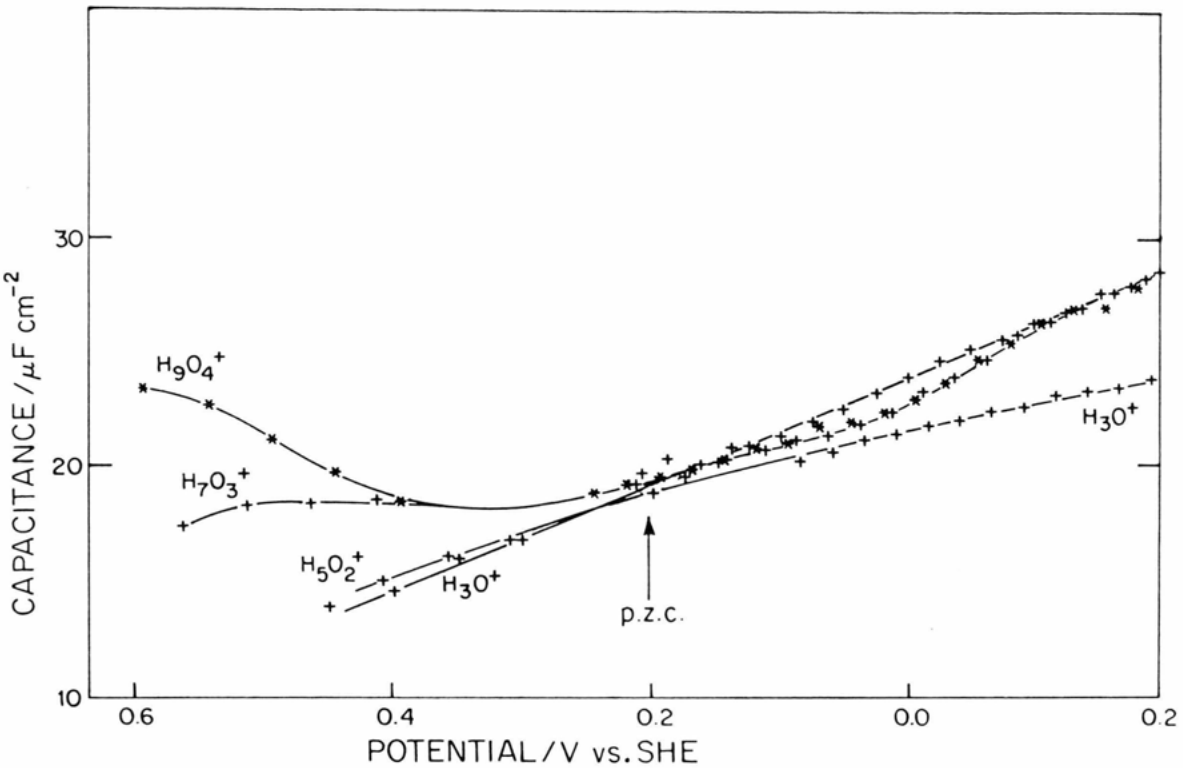

Fig. 5. Comparative plot of the capacitance behaviour of the Hg-pool electrode in the various proton-hydrate/$CF_3SO_3^-$ systems.

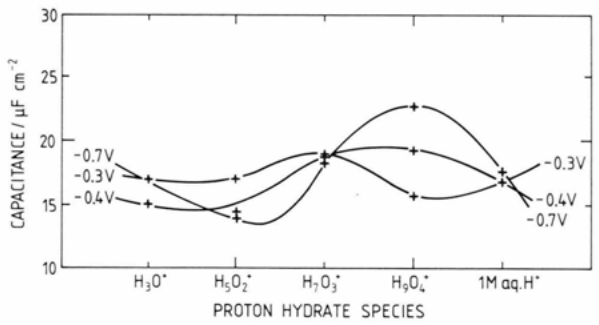

Fig. 6. Capacitance values for the Hg-pool electrode as a function of proton-hydrate speciation at the 3 cathodic overpotentials −0.3 V, −0.4 V (vs. SHE) and −0.7 V (vs. RHE).

attributed presumably to the potential-dependence both of ε_c and d in the the equation for C_c.

At potentials positive to the p.z.c. at Hg, all the C_c vs. E curves are quite similar (Fig. 5) (except at extreme positive potentials where preoxidation of Hg tends to occur due to $Hg_2(CF_3SO_3)_2$ formation). This is understandable since the inner region of the compact layer then tends to become populated with $CF_3SO_3^-$ anions (for the special situation in the H_3O^+ melt, see the double-layer structure diagram, Fig. 12 later).

3. *Capacitance Behaviour at Au in the Proton Hydrates*

At this point, it is convenient to compare the above results with those for Au, as a function of proton hydrate speciation.

The capacitance behaviour at Au in the various proton-hydrate solutions is shown as a function of potential in Figs. 7 a–d for the potential range 0 to 1.8 or 2.0 V vs. RHE, positive to the RHE potential in the same respective solutions.

Previous work at Au in aq. H_2SO_4 and $HClO_4$ showed [35] that regions of potential-dependent capacitance precede the initial stage of surface oxidation by 0.8 V or more and hence represent a stage of "pre-oxidation" of the Au surface by partial discharge of the anion. Similar effects are found for the behaviour in the $CF_3SO_3^-$ proton hydrate systems. Thus, from cyclic-voltammograms taken at sensitive

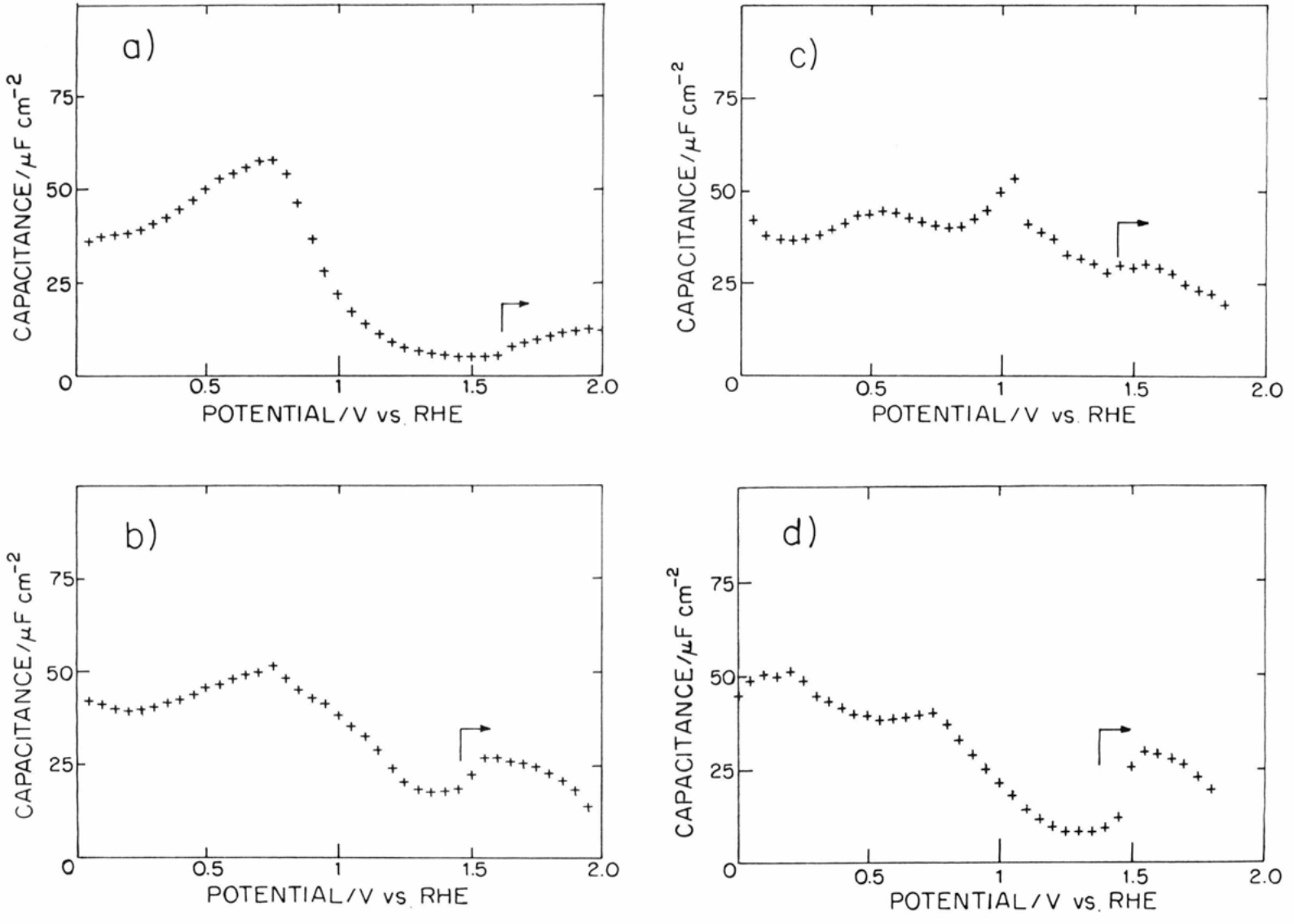

Fig. 7. Capacitance vs. potential profiles for the Au electrode in the proton hydrate systems as determined by small-amplitude cyclic linear sweeps on successive potential steps into the region of commencement of surface oxidation: a) H_3O^+; b) $H_5O_2^+$; c) $H_9O_4^+$ and d) 1.0 M aq. solution of CF_3SO_3H.

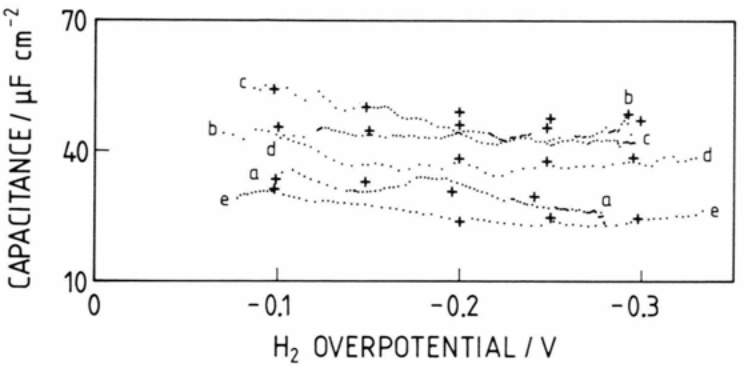

Fig. 8. Interfacial capacitance behaviour of Au at potentials negative to the RHE in the proton-hydrate media determined by means of a.c. impetance (+) and potential-relaxation methods (·····):
a) $H_3O^+ \cdot CF_3SO_3^-$;
b) $H_5O_2^+ \cdot CF_3SO_3^-$;
c) $H_7O_3^+ \cdot CF_3SO_3^-$;
d) $H_9O_4^+ \cdot CF_3SO_3^-$ and
e) 1 M aq. solution of CF_3SO_3H.

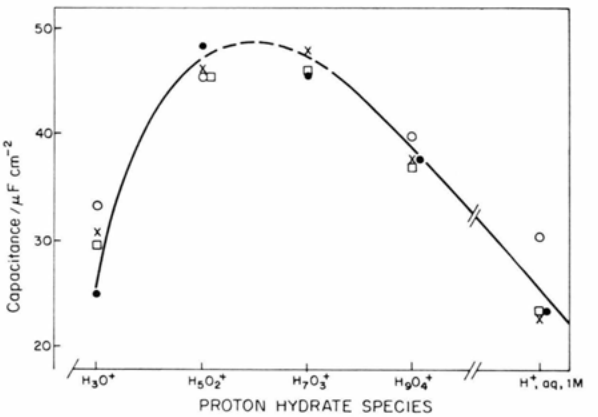

Fig. 9. Dependence of capacitance of the Au electrode at four potentials vs. RHE on proton-hydrate speciation (compare Fig. 6 for Hg). (○) −0.1; (×) −0.2; (□) −0.25; (●) −0.3 V vs. RHE.

current scales, it is possible to estimate the extent of charge-transfer, δq, associated with the pseudocapacitance due to anion chemisorption in the potential range +0.15 to 1.27 V, RHE for the case of the $H_3O^+ \cdot CF_3SO_3^-$ melt; from the cathodic and anodic sweeps, the values of δq are found to be 23 and 23 μC cm^{-2}, taking the three trigonal O atoms in the $CF_3SO_3^-$ as occupying 3 Au sites (cf. [35] for HSO_4^- and ClO_4^-). From these data, it can be concluded that there must be an appreciable degree of charge transfer of at last 0.5 e per anion, allowing for the possibility that some H_3O^+ ions also populate the interface at these positive potentials, i.e. the coverage fraction by $CF_3SO_3^-$ may be somewhat less than unity, especially in the H_3O^+ melt.

At other degrees of hydration of H^+, it is more difficult to distinguish the adsorption pseudocapacitance contribution due to anion chemisorption from the background electrostatic interfacial capacitance, but approximate values of δq of 20 to 25 μC cm^{-2} may again be estimated.

For potentials on the cathodic side of the H_2 reversible potential at Au, Fig. 8 shows the capacitance behaviour as a function of cathodic H_2 overpotential from −0.1 to ca. −0.35 V, determined by means of a.c. impedance and potential-relaxation measurements [27, 34, 36]. These two methods give results in quite good agreement, mostly to within 1 ~ 2 μF cm^{-2}.

The dependence of the capacitance at Au at H_2 overpotentials of −0.1 to −0.3 V on proton-hydrate speciation is shown in Figure 9. Here it is clear that a) a single maximum arises between the states $H_5O_3^+$ and $H_7O_3^+$ and b) that the C_c value for the $H_3O^+ \cdot CF_3SO_3^-$ melt is quite close to that for the 1 M aq. H_3O^+ solution, the values being ca. 25 and 24 μF cm^{-2}, respectively. The data points for potentials in the H_2 evolution region were evaluated by a.c. impedance at various potentiostatically held polarization potentials and from analysis of potential relaxation transients after polarization [27, 36].

At Au it is evident that the maximum value of C_c (about 48 μF cm^{-2} between $H_5O_2^+$ and $H_7O_3^+$) is about twice the values, 24 and 25 μF cm^{-2}, at the two ends of the curve. This difference is larger than those at Hg (Fig. 6). At Au, the data plotted are for −0.1 to −0.3 V vs. RHE while for Hg (Fig. 6) the data were plotted for three potentials −0.3, −0.4 V vs. SHE and −0.7 V vs. RHE.

Comparison of Capacitance Values at Hg and Au in the H_3O^+ Melt and for 1 M aq. H^+

A comparative tabulation of actual values of C for Hg and Au at potentials negative to the RHE is given in Table 1.

For the data in the H_2 evolution potential range (−0.1 to −0.3 V RHE), the main point of interest is

Table 1. Interfacial capacitance values for polycrystalline Au wire and liquid Hg at 313 K in solutions of the proton in various states of hydration.

Nominal state of the hydrated proton	Capacitance value/μF cm^{-2} *				
	H_3O^+	$H_5O_2^+$	$H_7O_3^+$	$H_9O_4^+$	1 M aq. solution
Electrode potential vs. RHE/V at Au					
−0.10	33.3	45.6	53.4	(40)	30.6
−0.20	30.9	46.0	47.9	37.9	23.0
−0.25	29.6	45.4	46.0	37.0	23.7
−0.30	(25)	48.4	45.8	37.8	23.8
Electrode potential vs. RHE at Hg					
−0.5				17.6	
−0.55		16.7	17.9	18.4	
−0.6	19.3	15.9	18.5	19.7	15.7
−0.65		14.4	18.3	21.1	16.3
−0.7	16.7	13.8	18.2	22.7	17.5
−0.75	16.0		17.3	23.4	19.0
−0.8	14.9				20.4

* Uncertainties in these values are ca. 0.5 μF cm^{-2}.

that the interfacial capacitance values lie in the range 25 to 33 μF cm^{-2} for Au in the H_3O^+ molten salt, quite close to the range of values, 24 to 31 μF cm^{-2}, found for 1 M aq. solutions (Table 1) where the values for Hg are in the range 16 ~ 20 μF cm^{-2}. The potentials in the range covered in this Table and Fig. 6 are some 0.5 to 0.7 V negative to the p.z.c. of Au (in dilute solutions), so are probably not influenced by the chemisorption of $CF_3SO_3^-$ indicated from Figs. 7a–d. The surprising result therefore seems to be that the capacitance is determined principally by the contact distance between H_3O^+ and the Au surface, independent of the influence of closely surrounding $CF_3SO_3^-$ anions in the melt or of water molecules in the aqueous solution case (column 6, Table 1), the difference between the data at the same respective potentials being only ca. 10 ~ 15%. However, the changing state of hydration of the proton in going from H_3O^+ to the fully aquated proton, through the intermediate states $H_5O_2^+$, $H_7O_3^+$, evidently does have a substantial effect on the capacitance at cathodic overpotentials, with maximum values being exhibited around a degree of hydration corresponding to "$H_7O_3^+$" (Fig. 9), with the ratio between the lowest and highest values being about 2, well outside the limits of error and reproducibility in the capacitance values determined by the two methods (Fig. 8). Also, the variations of C with state of hydration of the proton are reasonably consistent for all four cathodic potentials for which data were acquired at Au (Fig. 9); at Hg, the data show some variability with speciation but this is not due to experimental error.

In dilute aqueous medium, values of C_c greater than the value of ca. 17 μF cm^{-2} found at Hg for potentials negative to the p.z.c., arise at e.g. Ga [37]. Schmickler has treated this matter and shown [38] that values of C_c significantly larger than those at Hg can be accounted for in terms of the free electron density in the metal. However, it is difficult to adduce this as the reason for the 48 μF cm^{-2} value for Au in ca. $H_7O_3^+$ medium since lower values at *the same metal* are found in H_3O^+ medium and 1 M aq. media (Table 1 and Fig. 9). Hence the high C values for intermediate states of hydration of H^+ must be attributed to the specific extent of solvation of the proton coupled with the co-anion concentration. While the above difference for Au must be due to the different states of proton hydration, Table 1 shows that there is, however, a systematically larger series of values of C at Au than at Hg for respective proton hydrate species. It is this effect that could be caused by the different free electron density at Au than Hg.

We have referred to various proton-hydrate species in discussion of the above results. Apart from H_3O^+ in the $H_3O^+ \cdot CF_3SO_3^-$, the stoichiometries of the hydrates will be time-average ones. That they have some reality in terms of stability is indicated by their observation in vapour-phase experiments in the mass-spectrometer by Knewstubb and Tichner [39], as illustrated in Fig. 10.

4. Comparison with Double-Layer Capacitance Behaviour in Simple Alkali Halide Molten Salts

The work of Ukshe et al. [23] on double-layer capacitance behaviour at a molten Pb electrode in alkali-halide melts at elevated temperature enables an interesting comparison to be made with the present results on the molten $H_3O^+ \cdot CF_3SO_3^-$ salt measured at 313 K. The behaviour observed in the $H_3O^+ \cdot CF_3SO_3^-$ melt at Hg or Au is quite contrary to that reported for Pb in the molten alkali-metal salts at high temperature in the above work, where a sharp minimum around the p.z.c. of Pb is observed, reminiscent of the potential-dependence of the diffuse-layer capacitance in dilute aqueous solutions, although there can, of course, be no diffuse-layer in the interphasial region of a molten salt in contact with an electrode but probably rather an oscillatory charge-

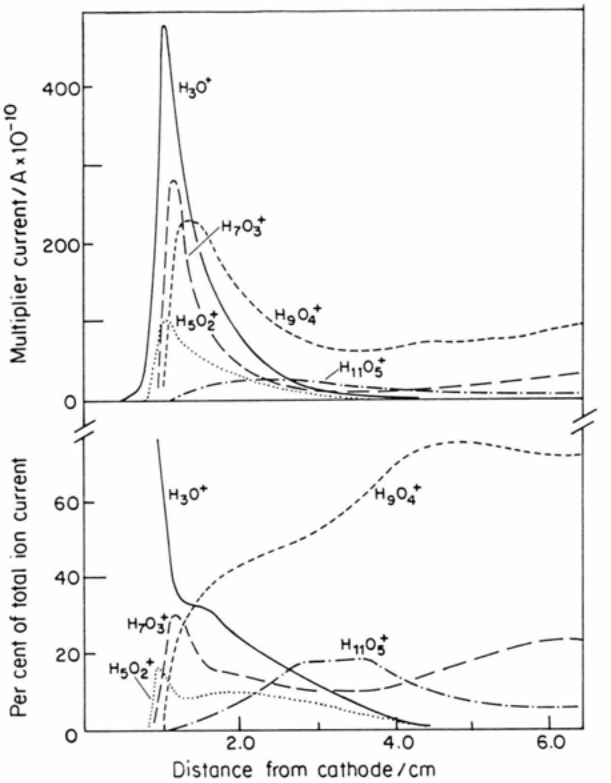

Fig. 10. Speciation of proton hydrates in vapour-phase mass-spectrometric experiments (from Knewstubb and Tichner [37]).

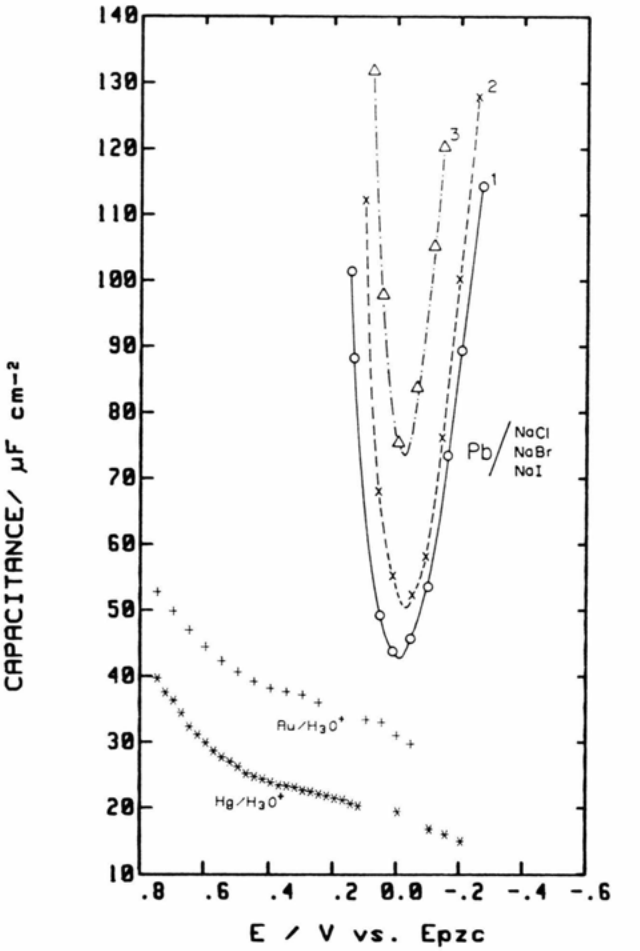

Fig. 11. Capacitance vs. potential profiles for a Pb electrode, around its p.z.c. in molten NaCl, 1093 K (curve 1); NaBr, 1073 K (curve 2) and NaI, 1073 K (curve 3), together with comparative plots for Hg and Au in $H_3O^+ \cdot CF_3SO_3^-$ at 313 K.

distribution over several ionic diameters away from the interface. It was suggested that the distribution of detects in the melt (cf. [23]) could behave analogously to a diffuse-layer, the Debye-Hückel ionic atmosphere giving large diffuse-layer type capacitance values around the p.z.c. However, such values should combine in the usual way with a short-range Helmholtz-layer capacitance giving rise to limits of the rise of the quasi-diffuse-layer capacitance as potentials sufficiently divergent from the p.z.c. are covered. This is not the case for the molten alkali-halides, where C rapidly increases in an exponential or parabolic way, away from the p.z.c., as illustrated in Fig. 11, while the data for Hg and Au show no such minimum (see also Fig. 11).

5. Double-Layer Structure in the Proton Hydrate Media

The transition in configuration of the double-layer which must arise through increasing degrees of hydration of $H_3O^+ \cdot CF_3SO_3^-$ is expected to be substantial; it can be qualitatively illustrated in the schematic way shown in Fig. 12. In the melt, at appreciable negative charge densities on the electrode, the charge distribution must approach, locally, that of a triple layer: $M^-H_3O^+A^-$; Fig. 12a. As more water is associated with the proton (it will be preferentially associated with the latter ion since $CF_3SO_3^-$ is a large anion), water of hydration of H_3O^+ will appear in the inner-layer together with some solvent-shared ion pairs nearby (Fig. 12b); in excess water (H^+ aq., Fig. 12c), the normal situation of an outer Helmholtz plane, populated by H_3O^+, together with an inner layer of

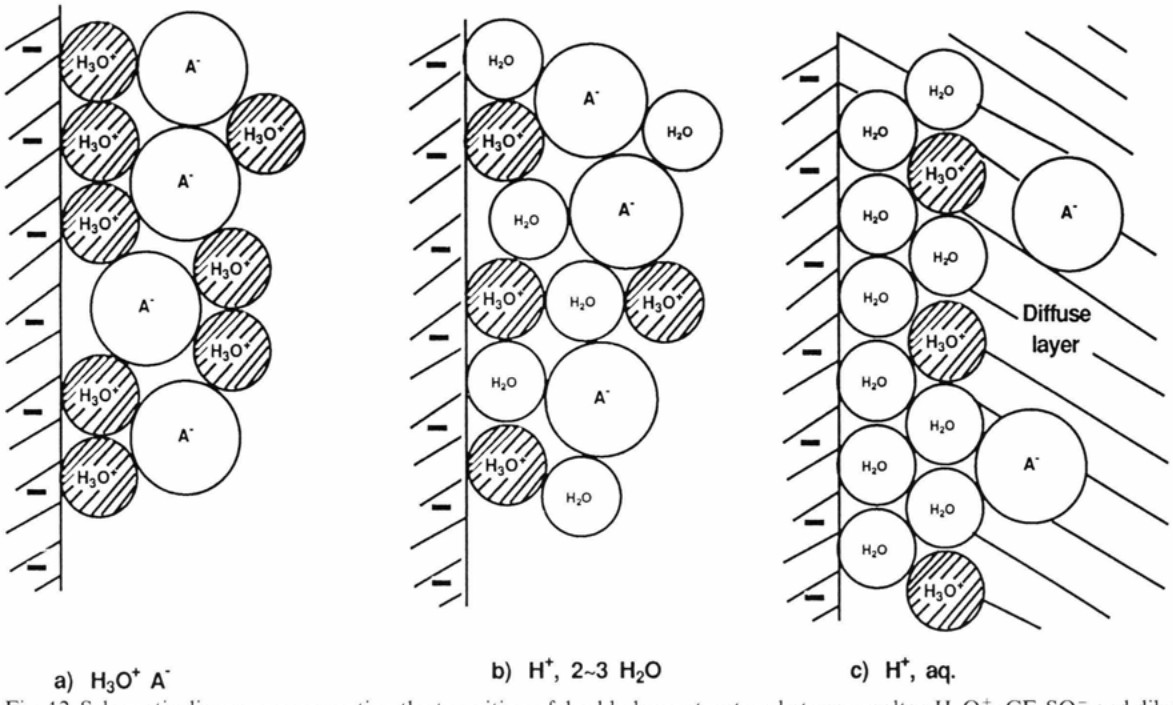

Fig. 12. Schematic diagrams representing the transition of double-layer structure between molten $H_3O^+ \cdot CF_3SO_3^-$ and dilute aq. solutions of H^+.

oriented H_2O dipoles [2, 3], may be assumed to arise, but note that, statistically, some conversion of inner-layer H_2O molecules to H_3O^+ will be able to occur through the usual proton-hopping mechanism [17, 18]. Since however, the compact layer capacitance at Hg is similar for aqueous acid solutions to those of NH_4^+ and K^+ ions of similar radii, the preferred time-average location of H_3O^+ is clearly in the outer Helmholtz plane.

The two extreme structures of the double-layer suggested in Fig. 12a and c, represent very different electrostatic situations: limitingly a "triple-layer capacitor", $-+-$, in Fig. 12a and the usual series combination [5] of a dipole capacitance [2, 3] with an ionic/electronic charge capacitance: $1/C_c = 1/C_{dipole} + 1/C_{Helmholtz}$, in Fig. 12c.

We have mentioned, in Sect. 4, that the capacitance results show a remarkable difference in behaviour from those determined by Ukshe et al. [23] in molten inorganic salts, e.g. NaCl, NaBr, NaI, at a molten lead electrode around 1073–1093 K (Fig. 11) where a relatively sharp minimum arises in C at or near the p.z.c., the minimum values in C being in the range 30 to 75 $\mu F\,cm^{-2}$, depending on the anion of the salt. The present results for the melt $H_3O^+ \cdot CF_3SO_3^-$ show *no* significant minimum in the whole experimental potential range -0.3 V to 1.3 V RHE at Au or -0.8 V to $+0.35$ V RHE at Hg, beyond which positive potentials surface oxidation commences. Of course, the behaviour found by Ukshe et al. [23], although similar to that observed at Hg around the p.z.c. in dilute solutions, cannot arise for the same reasons involving properties of a Gouy-Chapman diffuse layer [5, 7].

In the present examples of the behaviour of proton hydrates at Au, earlier results showed [40] that at potentials positive to the RHE in the same medium, specific adsorption of the anion $CF_3SO_3^-$ dominates the capacitance behaviour over the potential region (ca. $+0.5 \pm 0.1$ V, RHE) where the p.z.c. is otherwise expected to arise, so that this may be the reason why no minimum is observed. This may also be due to the much lower temperature than that in the work of Ukshe et al. [23], which will favour anion adsorption, or to H-bonding in the present case of $H_3O^+ \cdot CF_3SO_3^-$.

In the media containing further water molecules, up to $H_3O^+ + 3H_2O$ ($H_9O_4^+$), the interfacial capacitance at the potentials negative to the RHE becomes almost

doubled. Although the double-layer will then be populated by water-separated ion pairs which increase the distance of the H_3O^+ layer from the metal surface, the dielectric constant may be sufficiently increased by the additional water present that the resulting capacitance is substantially larger. Obviously this is determined in a rather inaccessible way by the ratio ε/d, where both ε and d can be changing. Under the conditions of restricted water content, a free H_2O dipole capacitance [3] in the inner layer is unlikely to be developed (as it is in dilute solutions) owing to the strong solvational binding of H_2O molecules between H_3O^+ and $CF_3SO_3^-$ (solvent-separated ion pairs). Also the proton charge can become diffused between the 2, 3 and 4 water molecules of hydration [17, 18] hydrogen bonded to H_3O^+. In the extreme of excess water (1M aq. H^+), the situation at potentials cathodic to the RHE is presumably represented by conventional models [3, 5].

6. *Numerical Values of the Capacitance in the $H_3O^+ \cdot CF_3SO_3^-$ Melt*

The numerical values of the capacitance both for the $H_3O^+ \cdot CF_3SO_3^-$ melt at Hg and Au and also for the molten-metal salts of [23] are unexpected high. Thus, one of the most interesting and seemingly surprizing results of the present work is the similarity of compact double-layer capacitance values, at potentials negative to the p.z.c. both for Hg and Au, for the two extreme states of hydration of the proton: H_3O^+ in the $H_3O^+ \cdot CF_3SO_3^-$, melt and H^+ aq. in 1 M aqueous CF_3SO_3H solution, as referred to earlier.

For ordinary dilute aqueous solutions, e.g. at Hg at potentials negative to the p.z.c. where [5] $C_c \approx 18\ \mu F\ cm^{-2}$, the application of simple electrostatics leads from this value of C_c to a physically reasonable value of ε for the compact layer region. Thus, with units of metres, $C = 1.8 \times 10^{-1}\ F\ m^{-2}$, the thickness, d, of the compact double-layer taken as its usually assumed value ca. 4.2×10^{-10} m $(= r_{H_3O^+} + 2\, r_{H_2O})$ and $\varkappa_0$, the permittivity of free space, taken as $8.85 \times 10^{-12}\ F\ m^{-1}$, we find, using the appropriate units,

$$\varepsilon = \frac{d\, C_c}{\varkappa_0} \doteqdot 8.5 . \qquad (1)$$

This is actually the more or less expected order of the value for ε in the compact layer at appreciable charge densities where (cf. [3, 41, 42]) significant saturation of the orientational polarization in ε can arise, giving values substantially less than the bulk, zero-field value, as in hydration shells around ions [43].

The fact that C_c for Hg or Au, at negative electrode charge-densities, is also ca. 16 $\mu F\ cm^{-2}$ for the H_3O^+ melt seems initially a surprising result since there is no dielectric fluid between either the H_3O^+ cations or the $CF_3SO_3^-$ anions and the Hg or Au metal surfaces. However, considering the C values for the H_3O^+ melt (Table 1) and assuming that the effective charge separation distance, d, across the interphase is equal to the radius, 0.138 nm, of the H_3O^+ ion, the resulting dielectric constant value would be ca. 3.2. Since, in the H_3O^+ melt, free water is absent, the above value seems phyically reasonable. For the higher hydrates, the effective interfacial separation of charges across the double-layer would be expected to be significantly larger than that for the H_3O^+ melt, e.g. by the diameter, 0.28 nm, of the H_2O molecule, but this will only tend to lower the value of C whereas, experimentally, for $H_7O_3^+$ and $H_9O_4^+$ media the capacities at Au are actually about twice that for H_3O^+. Bearing in mind, however, the shape and charge-distribution in the H_3O^+ ion [17, 19] the actual positive charge delocalized over the three protons could reside preferentially on one side of the trigonal pyramidal molecule ion so that the proton charge-density could come substantially nearer to the electrode surface of the electrode than would be indicated by the overall ionic diameter, but hardly less than the Bohr radius (ca. 0.1 nm) of the H atoms of H_3O^+. The electron-overspill effect at negative surface charge-densities would tend to enhance this effect. Although H_3O^+ is a fluxional molecule, like NH_3, proximity to the negatively charged electrode surface might be expected to lead to preferred orientation of the three protons on the metal side of the H_3O^+ ion. This would lead, with d now taken as ca. 0.1 nm, to $C \cong 22\ \mu F\ cm^{-2}$, close to the observed value at Hg (Table 1).

A tentative hypothesis might be that the $H_3O^+/CF_3SO_3^-$ ion pair polarization in the interphase, analogous to the Maxwell-Wagner effect, gives rise to a high value of C_c, fortuitously near that in dilute aqueous solutions but for a completely different reason.

A more quantitative examination of the significance of the C values for the higher proton hydrates at Hg or Au is difficult since as d tends to increase with increasing degree of hydration, ε will also tend to become larger as the fraction of water molecules

becoming rotationally freer (cf. [44]) in the interphase increases; thus C depends sensitively on the *ratio* ε/d, and both may be changing as we have remarked earlier.

7. *Kinetics of Proton Discharge at Au and Hg*

Using the series of proton hydrates, the electrode-kinetics of proton discharge was also evaluated. It may be expected that the kinetics of this process will be dependent on the state of hydration of the proton and on the structure of the double-layer in which the proton source resides. From Tafel polarization relations between current-density (i) and potential (V), the log [exchange current-densities, i_0], and the Tafel slopes, $b = \mathrm{d}V/\mathrm{d}\log i$, were evaluated in the usual way. The dependences of $\log i_0$ and b values for the H_2 evolution reaction at Au on speciations of the proton hydrate-$CF_3SO_3^-$ electrolytes are shown in Figure 13.

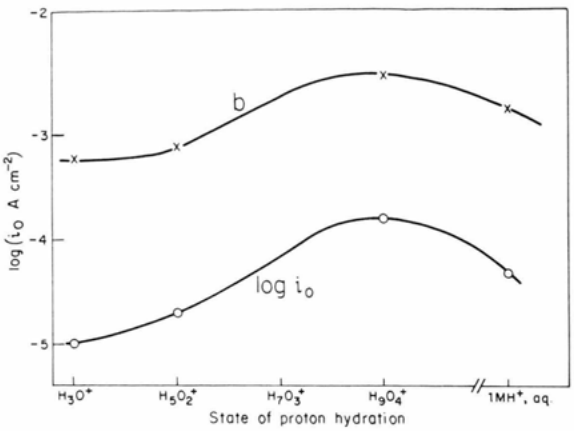

Fig. 13. Dependence of $\log i_0$ and b values for the H_2 evolution reaction at Au on the speciation of the proton hydrates.

For both Hg and Au, insignificant coverage of chemisorbed H, electro-deposited from the solvated proton, is observed. Hence, it is usually assumed that the step of proton discharge

$$e + H^+(nH_2O) + M(\text{Hg or Au}) \rightarrow MH_{ads} + nH_2O \quad \text{(I)}$$

is rate-determining for the overall reaction of H_2 formation which involves, as a second step, either the electrochemical desorption process

$$e + H^+(nH_2O) + MH_{ads} \rightarrow H_2 + nH_2O + M \quad \text{(II)}$$

or the catalytic recombination

$$2\,MH_{ads} \rightarrow H_2 + 2\,M\,. \quad \text{(III)}$$

Thus the kinetic parameters in Fig. 13 will refer to step (I). In considering the sequence of values of $\log i_0$, it must be remembered that there is a major increase in concentration from the 1 M aq. H^+ solution to the H_3O^+ melt (14 molal).

From experiments at various temperatures at Au, the Tafel b values at these temperatures can be compared. It is found, surprisingly, that the b values *decrease* with temperature, contrary to the expectations from conventional representations of $b = 2.3\,RT/\beta F$, where β, the barrier symmetry factor, is taken as a constant around 0.5.

These results provide a further interesting example (cf. [26]) of the commonly observed non-conventional variation of b with T due to a supposed variation of β with T. Thus, it has been proposed [26] that β is, in fact, represented by the relation $\beta = \beta_H + T\beta_S$, where β_H is an enthalpic and $T\beta_S$ an entropic component of β, representing the effect of electrode potential on the Gibbs energy of activation of the proton discharge process. Here, in order to understand the unusual decrease of b with T, it is necessary to account for a negative value of $\mathrm{d}b/\mathrm{d}T$ in the above expression for $b\,(= 2.3\,RT/[\beta_H + \beta_S T]F)$. From this latter relation, $\mathrm{d}b/\mathrm{d}T$ follows obviously as

$$\mathrm{d}b/\mathrm{d}t = 2.3\,R\beta_H/(\beta_H + T\beta_S)^2\,F. \quad (2)$$

β can never be negative since it represents the direct effect of potential on the energy of activation ($\Delta H_V^{\ddagger} = \Delta H_{V=0}^{\ddagger} - \beta_H VF$) which always decreases with increasing numerical value of the potential (in the negative direction for a cathodic process). Since the term $(\beta_H + T\beta_S)^2$ must always be positive*, it is clear that (2), based on the relation $\beta = \beta_H + T\beta_S$, can *never* account for the direction of change of b values with temperature for proton transfer at Au from the H_3O^+ melt or the $H_5O_2^+$ hydrate.

We have considered whether the observed behaviour could arise on account of a temperature-dependence of the pre-exponential transmission coefficient, $\varkappa$, in reaction kinetics since, formally, an apparent temperature-dependence of β corresponds [26, 45] to a potential-dependence of the entropy of activation, $\Delta S^{\ddagger}$, of the process. A potential-dependence of $\varkappa$ could correspond to an apparent potential-depen-

* The only formal possibility for $\mathrm{d}b/\mathrm{d}T$ to be negative is if the T factor within the $\beta_H + T\beta_S$ term in (2) has a power > 1. This is physically unlikely, as is also the possibility that β_S is itself proportional to T to a power > 0.

dence of the log of the frequency factor, i.e. of a component of the apparent $\Delta S^{\neq}$. However, this will appear also nominally as a β_S term, or a component of it, so again, on the basis of (2), could not account for negative values of db/dT.

For the above reasons, we must suppose that the negative db/dT arises from a temperature-dependent structural aspect of the double-layer in the H_3O^+ melt and for the $H_5O_2^+$ solution, connected e.g. with the potential profile across the region of distributed, partially hydrated H_3O^+ cations and $CF_3SO_3^-$ anions at the electrode interface, an effect which will presumably be dependent on electrode surface charge-density and on temperature.

Acknowledgement

Support of this work by the Natural Sciences and Engineering Research Council of Canada through the establishment of the Alcan-N.S.E.R.C.C. Research Chair of Electrochemistry at University of Ottawa is gratefully acknowledged.

[1] B. E. Conway and L. G. M. Gordon, J. Phys. Chem. **73,** 3523 (1969).
[2] R. J. Watts-Tobin and N. F. Mott, Electrochim. Acta **4,** 79 (1961).
[3] J. O'M. Bockris, M. A. V. Devanathan, and K. Müller, Proc. Roy. Soc. London **A 274,** 55 (1963).
[4] R. Parsons, J. Electroanal. Chem. **59,** 229 (1975).
[5] D. C. Grahame, Chem. Rev. **41,** 441 (1947).
[6] J. W. Schultze and F. D. Koppitz,. Electrochim. Acta **21,** 327, 337 (1976).
[7] O. Stern, Z. Elektrochem. **30,** 508 (1924).
[8] K. J. Vetter and J. W. Schultze, J. Electroanal. Chem. **44,** 63 (1973).
[9] W. Lorenz and G. Salie, Z. phys. Chem. Leipzig **29,** 390, 408 (1961).
[10] J. A. V. Butler, Proc. Roy. Soc. London **A 157,** 523 (1936).
[11] R. A. Marcus, J. Chem. Phys. **24,** 966 (1956); see also Ann. Rev. Phys. Chem. **15,** 155 (1964) and Biochim. Biophys. Acta **811,** 265 (1985).
[12] K. Heinzinger, Pure and Applied Chem. **57,** 1031 (1985).
[13] G. Nemethy and H. A. Scheraga, J. Chem. Phys. **36,** 3382, 3401 (1962).
[14] B. E. Conway, Ionic Hydration in Chemistry and Biophysics, Elsevier Publ. Co., Amsterdam 1981.
[15] E. Spohr and K. Heinzinger, J. Chem. Phys. **84,** 2304 (1986). – Ber. Bunsenges. phys. Chem. **92,** 1358 (1988). – Z. Naturforsch. **31a,** 463 (1976).
[16] P. Bopp, G. Jansco, and K. Heinzinger, Chem. Phys. Letters **98,** 129 (1983); see also Z. Naturforsch. **32a,** 1137 (1973); **31a,** 463 (1976).
[17] J. D. Bernal and R. H. Fowler, J. Chem. Phys. **1,** 515 (1933).
[18] B. E. Conway, J. O'M. Bockris, and H. Linton, J. Chem. Phys. **24,** 834 (1956).
[19] B. E. Conway, in: Modern Aspects of Electrochemistry, vol. 3, chapt. 2 (J. O'M. Bockris and B. E. Conway, eds.), Butterworths Sci. Publ., London 1964.
[20] R. P. Bell, The Proton in Chemistry, Cornell Univ. Press, Ithaca, New York 1959.
[21] M. Eigen and J. de Maeyer, Proc. Roy. Soc. London **A 247,** 505 (1958); see also E. Wicke, M. Eigen, and T. Ackermann, Z. phys. Chem. N.F. **1,** 342 (1954) and T. Ackermann, Discussions Faraday Soc. **24,** 180 (1957).
[22] B. E. Conway and D. F. Tessier, Intl. J. Chem. Kinetics **13,** 925 (1981).
[23] E. Ukshe, N. G. Bukun, D. I. Leikis, and A. N. Frumkin, Electrochim. Acta **9,** 431 (1964).
[24] B. E. Conway, D. J. MacKinnon, and B. V. Tilak, Trans. Faraday Soc. **66,** 1203 (1970).
[25] B. E. Conway and D. P. Wilkinson, J. Electroanal. Chem. **214,** 633 (1986).
[26] B. E. Conway, in: Modern Aspects of Electrochemistry, vol. 16, chapt. 2 (B. E. Conway, J. O'M. Bockris, and R. E. White, eds.), Plenum Publ. Corp. New York 1985.
[27] B. E. Conway and T. C. Liu, J. Chem. Soc. Faraday Trans. I, **83,** 1063 (1987).
[28] H. A. Kozlowska, B. E. Conway, and W. B. A. Sharp, J. Electroanal. Chem. **43,** 9 (1973).
[29] B. E. Conway, H. A. Kozlowska, W. B. A. Sharp, and E. Criddle, Anal. Chem. **45,** 1331 (1973).
[30] H. A. Kozlowska, B. Barnett, B. E. Conway, and J. Mozota, J. Electroanal. Chem. **100,** 417 (1979).
[31] E. R. Andrew and R. Bersohn, J. Chem. Phys. **18,** 159 (1950).
[32] P. Kebarle, in: Modern Aspects of Electrochemistry, vol. 11, chapt. 1 (B. E. Conway and J. O'M. Bockris, eds.), Plenum Publ. Co., New York 1974.
[33] J. O'M. Bockris, in: Modern Aspects of Electrochemistry, vol. 1, chapt. 4 (J. O'M. Bockris, ed.), Butterworths, London 1954.
[34] B. E. Conway and L. Bai, Electrochim. Acta **31,** 1013 (1986).
[35] H. A. Kozlowska, B. E. Conway, A. Hamelin, and L. Stoicoviciu, Electrochim. Acta **31,** 1051 (1986).
[36] J. A. V. Butler and J. F. Armstrong, Trans. Faraday Soc. **29,** 1261 (1933).
[37] B. B. Damaskin and A. N. Frumkin, Electrochim. Acta **19,** 173 (1974); see also R. Parsons, J. Electroanal. Chem. **59,** 229 (1975).
[38] W. Schmickler, J. Electroanal. Chem. **150,** 19 (1983).
[39] B. Knewstubb and A. Tichner, J. Chem. Phys. **36,** 674 (1962); **38,** 464 (1963).
[40] B. E. Conway and S. Qian, Electrochim. Acta, in press (1990).
[41] B. E. Conway, J. O'M. Bockris, and I. A. Ammar, Trans. Faraday Soc. **47,** 756 (1951). – B. E. Conway, Ph.D. thesis, Univ. of London 1949.
[42] D. C. Grahame, J. Chem. Phys. **18,** 903 (1950).
[43] W. M. Noyes, J. Amer. Chem. Soc. **84,** 513 (1962); **86,** 971 (1964).
[44] C. H. Collie, J. B. Hasted, and D. M. Ritson, J. Chem. Phys. **16,** 1 (1948).
[45] B. E. Conway, D. P. Wilkinson, and D. F. Tessier, J. Electrochem. Soc. **136,** 2486 (1989).